Cell Reports, Volume *24*

Supplemental Information

Antigen-Presenting Cell-Intrinsic PD-1 Neutralizes PD-L1 in *cis* to Attenuate PD-1 Signaling in T Cells

Yunlong Zhao, Devin L. Harrison, Yuran Song, Jie Ji, Jun Huang, and Enfu Hui

Supplemental Information

Supplemental figures and tables

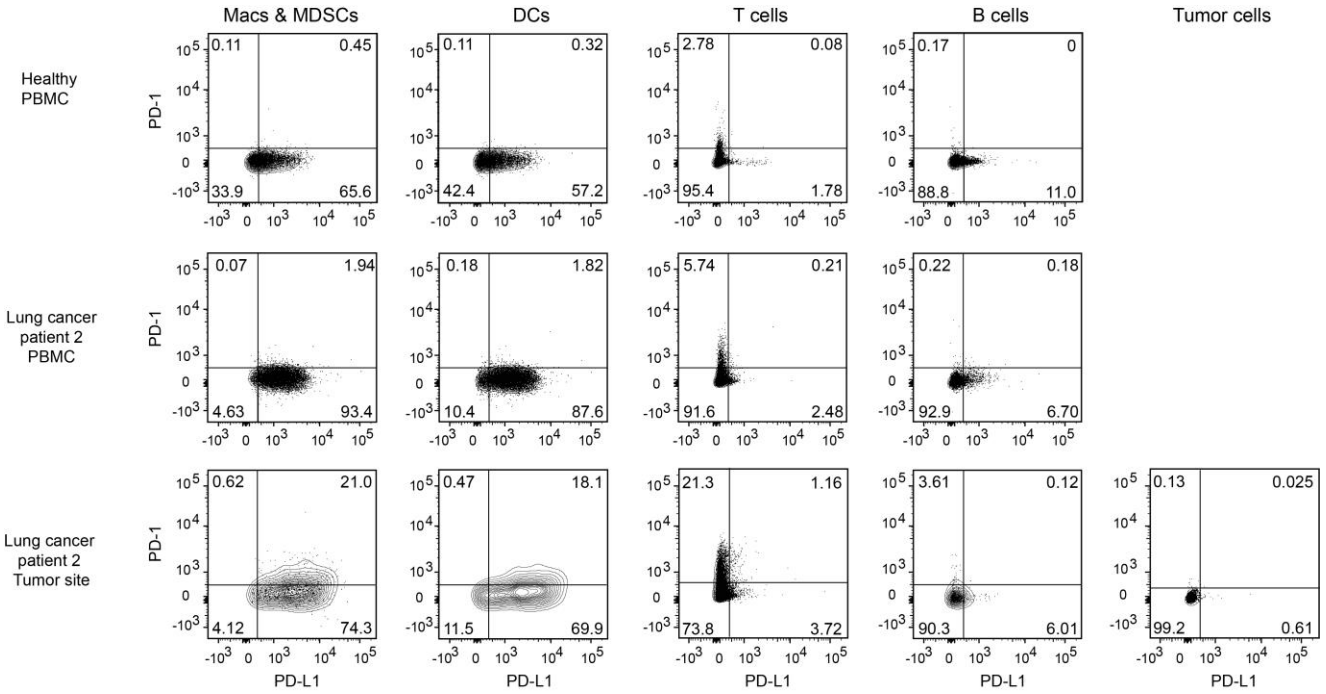

Figure S1 PD-1 and PD-L1 co-expression in the tumor microenvironment of a second lung cancer patient. Related to Figure 1. Expression of PD-1 and PD-L1 on the indicated cell types derived from PBMCs of a healthy human individual, from PBMCs of a lung cancer patient, and from the tumor site of the same patient. Both the healthy and lung cancer samples are from a different individual than in **Figure 1**. Cells were gated as described in **Figure 1A**.

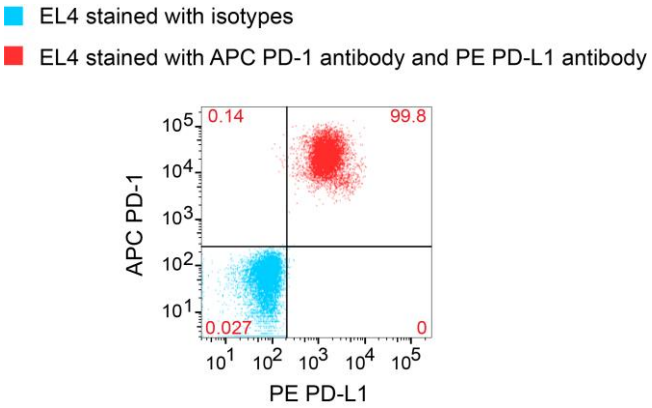

Figure S2 PD-1 and PD-L1 co-expression on EL4 cells. Related to Figure 1. Flow cytometry scatter plot showing 99.8% EL4 cells express both PD-1 and PD-L1. Cells double stained with PD-1 and PD-L1 antibodies are shown in red, and cells double stained with the respective isotype antibodies are shown in blue.

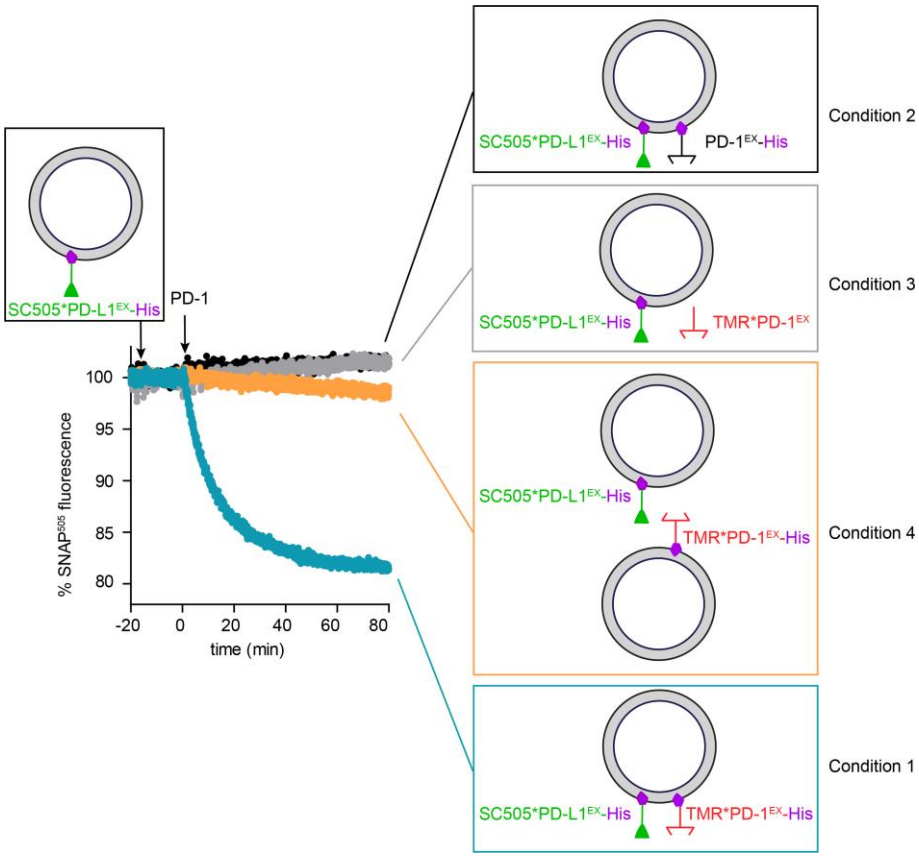

Figure S3 PD-L1 fluorescence is selectively quenched by *cis*-PD-1. **Related to Figure 3.** LUVs reconstituted with SC505*PD-L1^{EX}-His were added with TMR*PD-1^{EX}-His (condition 1), unlabeled PD-L1^{EX}-His (condition 2), TMR*PD-L1^{EX} lacking a His-tag (condition 3), or TMR*PD-1^{EX}-His pre-attached to another set of LUVs (condition 4), and the SC505 fluorescence was monitored in real time. Kinetic traces corresponding to the above four conditions are shown in blue, black, gray, and orange, respectively. The resulting geometric distribution of the proteins under each condition was illustrated in the box on the right. In condition 4, because SC505*PD-L1^{EX}-His and TMR*PD-1^{EX}-His were pre-attached to two different sets of LUVs, they could only interact with each other in *trans*. Hence this condition has allowed us to conclude that the contribution of *trans*-interaction in condition 1, and in experiments conducted in **Figure 3B**, was minor during the time course of the assay. Shown is one representative result from three independent replicates.

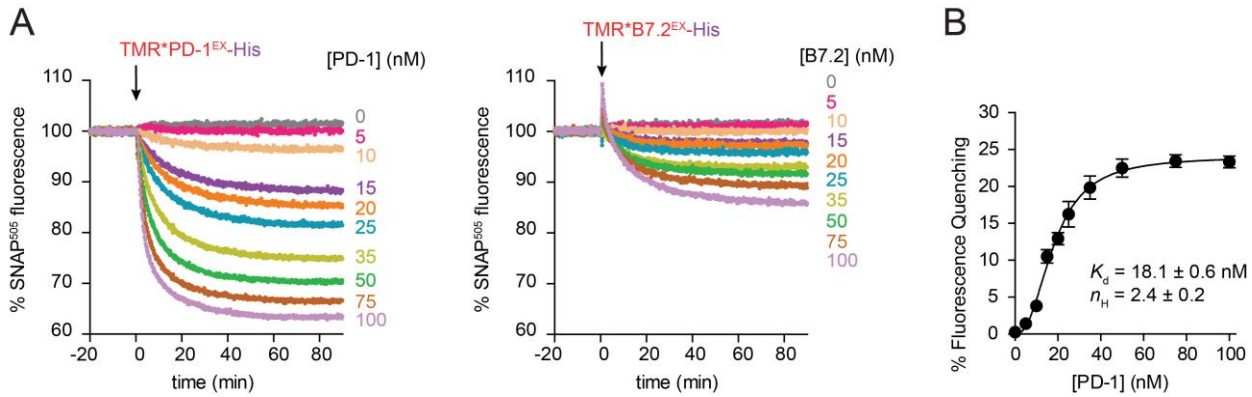

Figure S4 Quenching of PD-L1 fluorescence depends on the concentration of PD-1. Related to Figure 3.

(A) LUVs pre-bound with SC505*PD-L1^{EX}-His were added with increasing concentrations of TMR*PD-1^{EX}-His (Left) or equivalent concentrations of TMR*B7.2^{EX}-His (Right). Because B7.2 does not interact with PD-L1 in *cis* (**Figure 2A** and **Figure 3B**), TMR*B7.2^{EX}-His mediated quenching of SC505*PD-L1^{EX}-His reflects a molecular crowding effect, and was subtracted from the TMR*PD-1^{EX}-His signal to calculate the % quenching due to PD-1/PD-L1 *cis*-interaction. Shown is one representative result from three independent replicates.

(B) % quenching due to PD-1/PD-L1 *cis*-interaction, calculated from raw traces in **A**, was plotted as a function of TMR*PD-1^{EX}-His concentration. The data were fit with GraphPad Prism 5.0 using the "Specific binding with Hill Slope" model, yielding the dissociation constant (K_d) and Hill coefficient (n_H) of the PD-1/PD-L1 *cis*-interaction. Data are presented as mean ± SEM from three independent measurements.

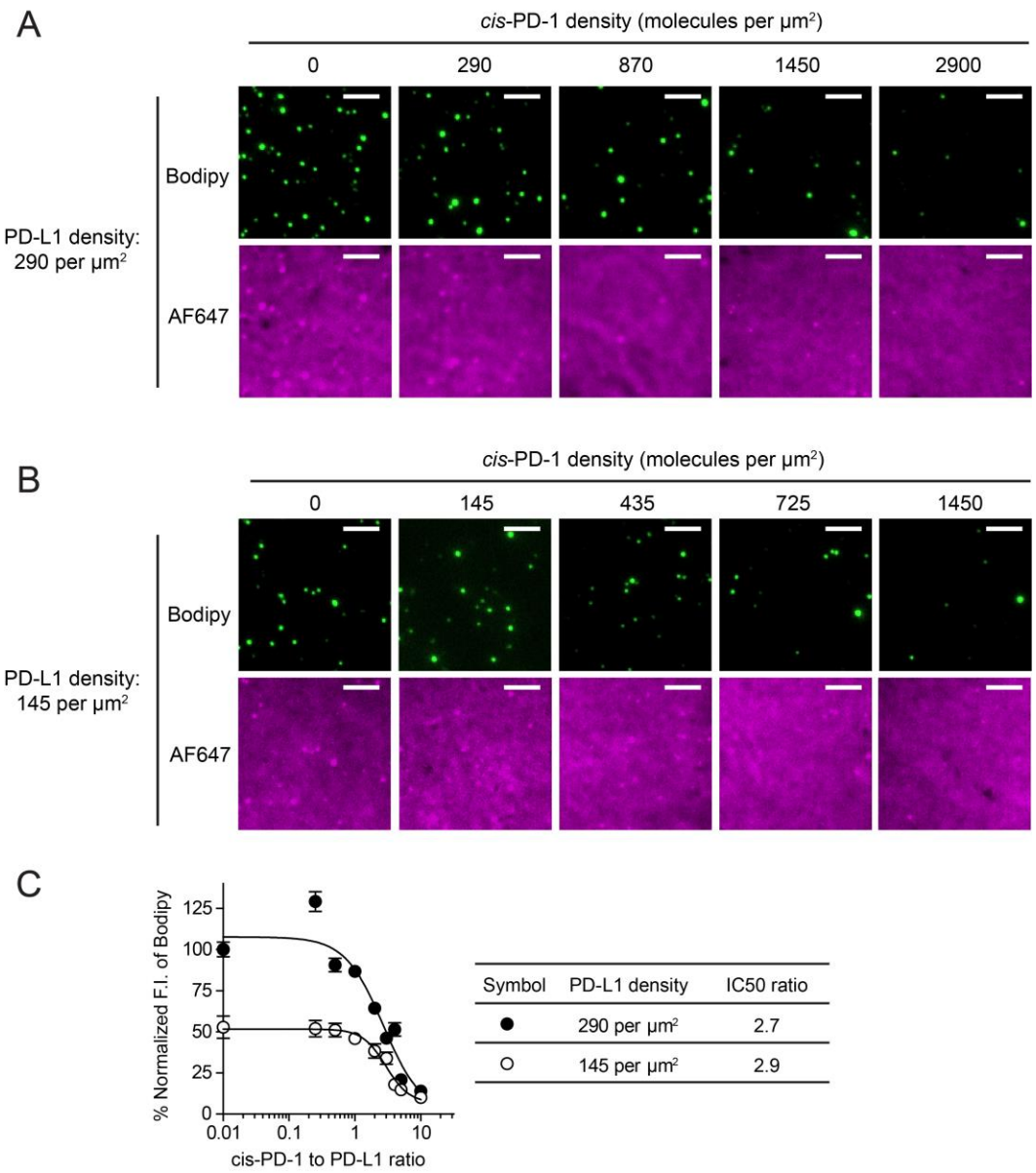

Figure S5 Titration of *cis*-PD-1 progressively inhibits PD-L1/PD-1 *trans*-interaction. Related to Figure 4.

(A) SC647*PD-1^{EX} coupled SLB was incubated with Bodipy/DGS-NTA-Ni LUVs carrying PD-L1^{EX} at 290 per μm^2 and *cis*-PD-1^{EX} at 0, 73, 145, 290, 580, 870, 1160, 1450, and 2900 per μm^2, as described in **STAR Methods**. Shown in the Bodipy channel are representative TIRF images of SLB-captured Bodipy LUVs at the indicated densities of *cis*-PD-1^{EX}. Shown in the AF647 channel are the respective SLB images. Scale bars: 5 μm.

(B) Same as (A) except lowering the LUV PD-L1^{EX} density to 145 per μm^2, and the *cis*- PD-1^{EX} densities to 0, 36, 73, 145, 290, 435, 580, 725, and 1450 per μm^2.

(C) The fluorescence intensity (F. I.) of Bodipy was normalized to the zero *cis*-PD-1 condition, and plotted as a function of *cis*-PD-1 to PD-L1 ratio, with the zero *cis*-PD-1 data plotted at ratio 0.01. The data were fit with GraphPad Prism 5.0 using the "Dose response - inhibition" model, yielding the 50% inhibition concentration (IC50). Data are presented as mean ± SEM from at least ten independent TIRF fields.

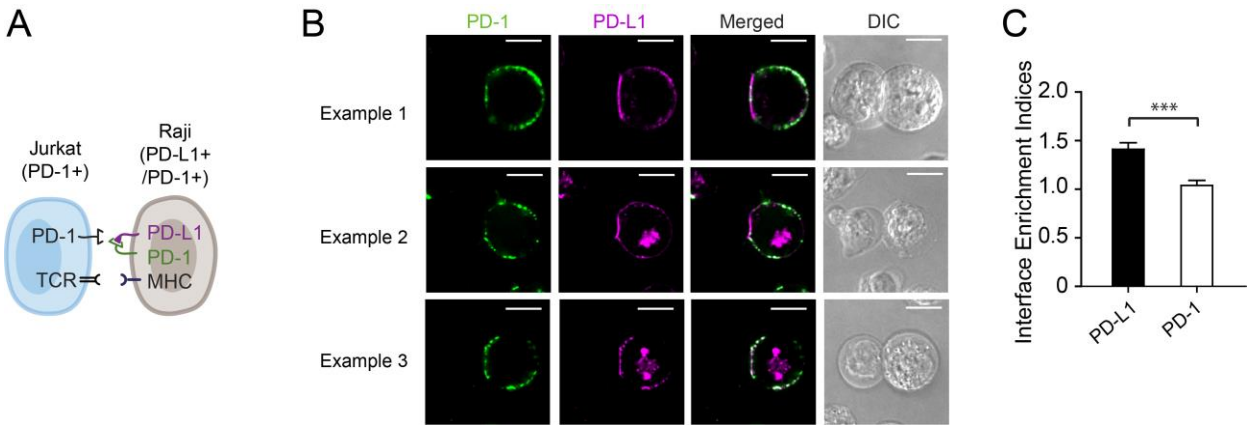

Figure S6 *Cis*-PD-1 on Raji APCs does not enrich to the interface. Related to Figure 6.

(A) A cartoon showing Raji co-transduced with PD-L1–mCherry (denoted as magenta PD-L1) and PD-1–mGFP (denoted as green PD-1) conjugated with Jurkat transduced with PD-1–SNAP (denoted as black PD-1).

(B) Confocal images of three representative Jurkat-Raji conjugates at indicated channels, acquired two minutes after the cell–cell contact. Scale bars: 10 μm.

(C) Bar graph summarizing the interface enrichment indices of both conditions shown in A. Mean ± SEM, n = 30 cells from three independent experiments.

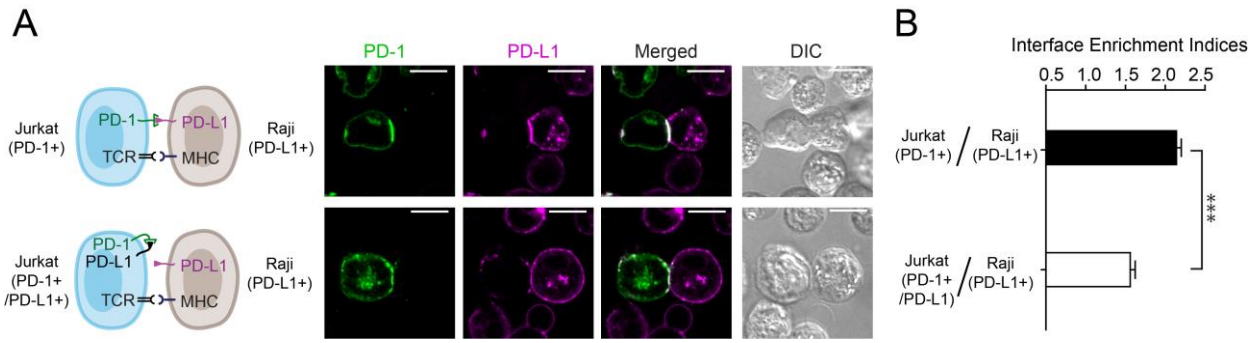

Figure S7 T cell PD-L1 inhibits the ability of T cell PD-1 to bind PD-L1 in *trans*. Related to Figure 6.

(A) Left, cartoons showing Raji transduced with PD-L1-mCherry (denoted as magenta PD-L1) conjugated with either Jurkat transduced with PD-1–mGFP (denoted as green PD-1) or Jurkat co-transduced with PD-1–mGFP and PD-L1. Right, representative confocal images of the Jurkat-Raji conjugates at the indicated channels, acquired two minutes after the cell–cell contact. Scale bars: 10 μm.

(B) Bar graph summarizing the interface enrichment indices of both conditions shown in **A**. Mean ± SEM, n = 35 cells from three independent experiments.

Table S1 Summary of PD-1 and PD-L1 surface expressions on various cells. Related to Figure 1.

Cell Type	Molecular density (molecules/μm2)	
	PD-1	**PD-L1**
NSCLC Tumor Cells	271	34
NSCLC B cells	297-350	10-13
NSCLC T cells	581-660	4-13
NSCLC DCs	138-172	32-43
NSCLC Macs & MDSCs	114-146	27-28
EL4	2975 ± 88	137 ± 17
HEK293T	72 ± 2	91 ± 5

Table S1 Summary of PD-1 and PD-L1 surface expressions on various cells. Related to Figure 1. Shown in this table are PD-1 and PD-L1 surface densities on NSCLC tumor cells, as well as NSCLC infiltrating B cells, T cells, DCs, Macs & MDSCs. Only the PD-1/PD-L1 double positive cells identified in **Figure 1** and **Figure S1** are quantified. Because no double positive tumor cells are found in patient 2 (**Figure S1**), we only report the values for patient 1 (**Figure 1**) here. Data of tumor infiltrating immune cells are reported as a range according to the expression levels in both patients. Data of EL4 and HEK293T are shown as mean ± SEM from three independent measurements.

Table S2 List of Oligos. Related to STAR Methods.

Name	Sequence	Note
EH-98	cctttccatgggtcttttctgcag atggacgctatgaagagag	clone signal peptide of HIV envelope glycoprotein into pPPI4, pair with EH-99
EH-99	ggtggctccatcggaatctagcatggat	clone signal peptide of HIV envelope glycoprotein into pPPI4, pair with EH-98
EH-100	tagattccgatggagccacccgcagttc	clone Strep-SNAP tag into pPPI4, pair with EH-101
EH-101	gtgatggaattcagattggaatcggacagtctcgctaccgctaccgctacctc	clone Strep-SNAP tag into pPPI4, pair with EH-100
EH-102	ttccaatctgaattccatcaccatcaccatcaccatcaccatcactgagcggc	clone His_{10} tag into pPPI4, pair with EH-103
EH-103	agctctagatgcatgctcgagcggccgctcagtgatggtgatg	clone His_{10} tag into pPPI4, pair with EH-102
EH-106	gactgtccgattccaatctggcgctcctctgaagattcaag	clone CD86 extracellular domain CDS into pPPI4, pair with EH-107
EH-107	gtgatggtgatggtgatggccaggaatgtggtctgggggag	clone CD86 extracellular domain CDS into pPPI4, pair with EH-106
EH-108	gactgtccgattccaatctggcccaggatggttcttagac	clone PD-1 extracellular domain CDS into pPPI4, pair with EH-109
EH-109	gtgatggtgatggtgatggcccaccagggtttggaactg	clone PD-1 extracellular domain CDS into pPPI4, pair with EH-108
EH-395	ctctagatgcatgctcgagctcacaccagggtttggaactg	clone PD-1 extracellular domain CDS without His_{10} tag into pPPI4, pair with EH-108
EH-110	gactgtccgattccaatctggctttactgtcacggttcccaag	clone PD-L1 extracellular domain CDS into pPPI4, pair with EH-111
EH-111	gtgatggtgatggtgatggccagtcctttcatttggagga	clone PD-L1 extracellular domain CDS into pPPI4, pair with EH-110
EH-247	gatcgataagcttgatatcg aggcaggcagaagtatgc	clone dSV40 to replace SFFV in pHR-PD-1-mGFP, pair with EH-248
EH-248	tgggatctgcatgagaattc agcctaggcctccaaaaaag	clone dSV40 to replace SFFV in pHR-PD-1-mGFP, pair with EH-247
EH-203	ggagctctcgagaattctcatgaggatatttgctgtctt	clone PD-L1 signal peptide into pHR, pair with EH-427
EH-427	atttcgcagtctttgtccattgcgttcagcaaatgccag	clone PD-L1 signal peptide into pHR, pair with EH-203
EH-428	atggacaaagactgcgaaatg	clone CLIP tag into pHR, pair with EH-429
EH-429	cacctccaccgctaccgctaccgctaccacccagcccaggcttgc	clone CLIP tag into pHR, pair with EH-428
EH-430	agcggtagcggtggaggtggaagcagctttactgtcacggttcccaag	clone PD-L1 into pHR, pair with EH-431
EH-431	caggtcgactctagagtcgcttacgtctcctccaaatgtgtatc	clone PD-L1 into pHR, pair with EH-430
EH-52	ggagctctcgagaattctcatgcagatcccacaggcg	clone PD-1 signal peptide into pHR, pair with EH-432
EH-432	atttcgcaatctttgtccatgaaccatcctggccgcca	clone PD-1 signal peptide into pHR, pair with EH-52
EH-433	atggacaaagattgcgaaatgaaac	clone SNAP tag into pHR, pair with EH-434
EH-434	cacctccaccgctaccgctaccgctacctcccagacccggtttacc	clone SNAP tag into pHR, pair with EH-433
EH-435	tagcggtagcggtggaggtggaagcagcttagactccccagacagg	clone PD-1 into pHR, pair with EH-436
EH-436	caggtcgactctagagtcgcttacaggggccaagagcagtg	clone PD-1 into pHR, pair with EH-435
EH-400	ggagctctcgagaattctcatgggactgagtaacattctc	clone CD86 signal peptide into pHR, pair with EH-440
EH-440	atttcgcaatctttgtccatagcaccagagagcaggaag	clone CD86 signal peptide into pHR, pair with EH-400
EH-441	tagcggtagcggtggaggtggaagcagcgctcctctgaagattcaagc	clone CD86 into pHR, pair with EH-442

EH-442	caggtcgactctagagtcgcttaaaaacatgtatcacttttgtcg	clone CD86 into pHR, pair with EH-441
EH-443	ttgggggccagggaggcggccccacagaggtaggtg	clone PD-1 I126A mutant into pHR, pair with EH-435
EH-444	gtggggccgcctccctggcccccaaggcgc	clone PD-1 I126A mutant into pHR, pair with EH-436
EH-464	ttgcggtaccgcgggcccgggatccaatggacaaagattgcgaaatg	clone SNAP to replace mGFP in pHR-PD-1-mGFP, pair with EH-465
EH-465	caggtcgactctagagtcgcggccgctttatcccagacccggtttacc	clone SNAP to replace mGFP in pHR-PD-1-mGFP, pair with EH-464
EH-203	ggagctctcgagaattctcatgaggatatttgctgtctt	clone PD-L1 into pHR to generate pHR-PD-L1-SNAP, pair with EH-516
EH-516	ttgatatcctgcagacgcgtcgtctcctccaaatgtgtatc	clone PD-L1 into pHR to generate pHR-PD-L1-SNAP, pair with EH-203
EH-483	acgcgtctgcaggatatcaag	clone SNAP into pHR to generate pHR-PD-L1-SNAP, pair with EH-465
EH-517	caccgacagcccaagtgaatgacca	synthesis DNA sequence of mouse PD-1 sgRNA to generate pX330GFP-mPD-1_1, pair with EH-518
EH-518	aaactggtcattcacttgggctgt	synthesis DNA sequence of mouse PD-1 sgRNA to generate pX330GFP-mPD-1_1, pair with EH-517
EH-519	caccgagttgagctggcaatcaggg	synthesis DNA sequence of mouse PD-1 sgRNA to generate pX330GFP-mPD-1_2, pair with EH-520
EH-520	aaacccctgattgccagctcaact	synthesis DNA sequence of mouse PD-1 sgRNA to generate pX330GFP-mPD-1_2, pair with EH-519

Table S3 List of Recombinant DNA. Related to STAR Methods.

DNA	SOURCE	IDENTIFIER
pMD2.G	Addgene	12259
psPAX2	Addgene	12260
pHR-PD-1-mGFP	Hui et al., 2017	N/A
pPPI4	Lee et al., 2015	N/A
pPPI4-Strep-SNAP-PD-L1-His_{10}	This paper	N/A
pPPI4-Strep-SNAP-PD-1-His_{10}	This paper	N/A
pPPI4-Strep-SNAP-PD-1	This paper	N/A
pPPI4-Strep-SNAP-CD86-His_{10}	This paper	N/A
pHR-CLIP-PD-L1	This paper	N/A
pHR-SNAP-PD-1	This paper	N/A
pHR-SNAP-PD-1 I126A	This paper	N/A
pHR-SNAP-CD86	This paper	N/A
pHR-dSV40-PD-1-mGFP	This paper	N/A
pHR-PD-1-SNAP	This paper	N/A
pHR-PD-L1-SNAP	This paper	N/A
pX330GFP-mPD-1_1	This paper	N/A
pX330GFP-mPD-1_2	This paper	N/A